

1

Supplementary Materials

2

Unveiling the Intrinsic Role of Water in the Catalytic Cycle of Formaldehyde Oxidation: A Comprehensive Study Integrating Density Functional Theory and Microkinetic Analysis

3

4

Qianyu Li^[a, b], Wenlang Li^[c, d], Jiachun Cao^[a, c, d], Junhui Zhou^[a], Didi Li^[c, d], and Zhimin Ao^{[a]*}

5

[a] Advanced Interdisciplinary Institute of Environment and Ecology, Beijing Normal University, Zhuhai 519087, PR China.

6

[b] School of Environment, Beijing Normal University, Beijing 100875, PR China

7

8

[c] Guangdong-Hong Kong-Macao Joint Laboratory for Contaminants Exposure and Health, Guangzhou Key Laboratory Environmental Catalysis and Pollution Control, Institute of Environmental Health and Pollution Control, Guangzhou 510006, PR China.

9

10

[d] Guangdong Key Laboratory of Environmental Catalysis and Health Risk Control, Key Laboratory for City Cluster Environmental Safety and Green Development of the Ministry of Education, School of Environmental Science and Engineering, Guangdong University of Technology, Guangzhou 510006, PR China.

11

12

13

Corresponding author's email address: is zhimin.ao@bnu.edu.cn.

14

15

Pages (9)

16

Table (1)

17

■ Table S1. The comparison of apparent energy (E_{apparent}) at 400 K and the energy of barrier (E_{bar}) of rate-determining step of $\text{Al}_1/\text{C}_2\text{N}$ and other reported catalysts.

18

19

Figures (7)

20

■ Fig. S1 The most stable configurations of (a) O_2 , (b) CO_2 , (c) H_2O , (d) N_2 , and (e) HCHO adsorbed on $\text{Al}_1/\text{C}_2\text{N}$.

21

■ Fig. S2 Three direct oxidation pathways of HCHO on $\text{Al}_1/\text{C}_2\text{N}$.

22

■ Fig. S3 The dissociating reaction of H_2O on $\text{Al}_1/\text{C}_2\text{N}$.

23

■ Fig. S4 Most stable configurations of (a) O_2 , (b) CO_2 , (c) H_2O , (d) N_2 and (e) HCHO adsorbed on hydrated $\text{Al}_1/\text{C}_2\text{N}$.

24

25

■ Fig. S5 Intermediate of HCHO degraded on hydrated $\text{Al}_1/\text{C}_2\text{N}$ and the relative energy and barrier energy for element reactions.

26

■ Fig. S6 Evolution of (a) relative energy (RE) and (b) temperature (T) of the $\text{Al}_1/\text{C}_2\text{N}$ with NVT AIMD simulation time and the geometric structures of the $\text{Al}_1/\text{C}_2\text{N}$ at simulation times (c) $t = 0$ ps and (d) $t = 2.5$ ps. The simulation temperature is 400 K.

27

28

■ Fig. S7 The reaction order of HCHO oxidation on $\text{Al}_1/\text{C}_2\text{N}$.

29

30

31

32

33 **Table S1. The comparison of apparent energy (E_{apparent}) at 400 K and the energy of**
 34 **barrier (E_{bar}) of the rate-determining step of $\text{Al}_1/\text{C}_2\text{N}$ and other reported catalysts.**
 35

Catalysts	E_{apparent} (eV)	
	Model predictions	Experimental data
LMO	1.00 (J. Ding et al., 2022)	0.94 (Xu et al., 2021) ^a
Sr-LMO	0.80 (J. Ding et al., 2022)	0.77 (Xu et al., 2021) ^a
Sn-LMO	0.80 (J. Ding et al., 2022)	
Ag-LMO	0.96 (J. Ding et al., 2022)	
$\text{MnCe}_{x-1}\text{O}_{2x-1}$ (111)	1.12 (W.Song et al., 2022)	
$\text{MnCe}_{x-1}\text{O}_{2x}$ (111)	1.60 (W.Song et al., 2022)	
$\text{Mn}_2\text{Ce}_{x-2}\text{O}_{2x}$ (111)	1.84 (W.Song et al., 2022)	
$\text{Mn}_3\text{Ce}_{x-3}\text{O}_{2x}$ (111)	2.54 (W.Song et al., 2022)	
$\text{Al}_1/\text{C}_2\text{N}$	1.30 (this work)	

Catalysts	E_{bar} (eV) of rate-determining step	
	Model predictions	Condition
$\text{Pd}/\text{Co}_3\text{O}_4$	0.90 (J. Deng et al., 2022)	Without H_2O
Co_3O_4 (defect)	1.37 (J. Deng et al., 2022)	Without H_2O
Co_3O_4 (perfect)	0.87 (J. Deng et al., 2022)	With H_2O
Co_3O_4 (defect)	0.51 (J. Deng et al., 2022)	With H_2O
$\text{Al}_1/\text{C}_2\text{N}$	0.86 (this work)	With H_2O

36 ^a Experimental condition: temperature = 110 °C, HCHO: O_2 = 1: 2000

37 ¹ Journal of Hazardous Materials 422 (2022) 126931

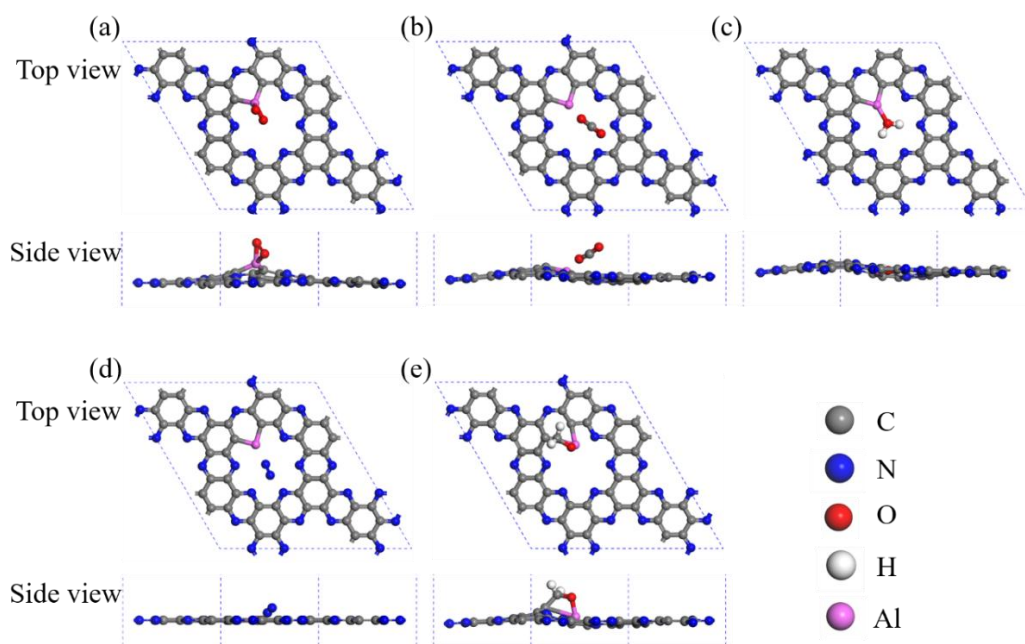
38 ² Appl. Catal. B 287, 119955.

39 ³ Journal of Hazardous Materials 425 (2022) 127985

40 ⁴ Catalysis Today 339 (2020) 210–219

41 ⁵ Chemical Engineering Journal 355 (2019) 540–550

42



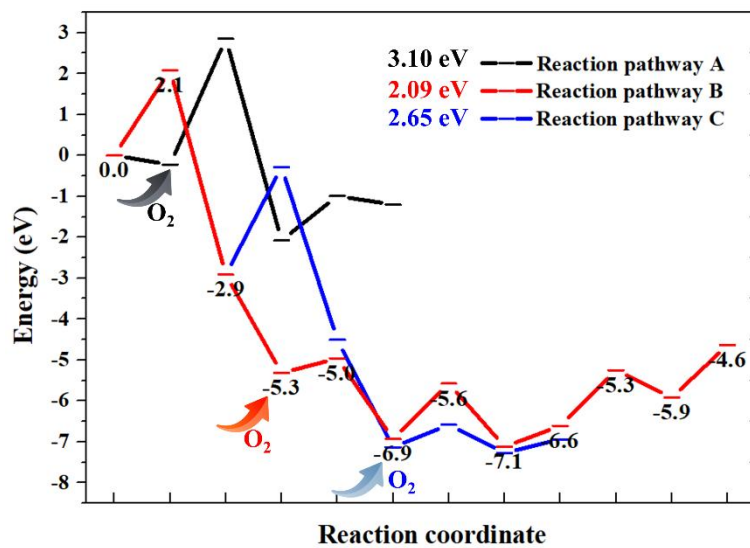
43

44 **Fig. S1 The most stable configurations of (a) O₂, (b) CO₂, (c) H₂O, (d) N₂, and (e) HCHO**

45

adsorbed on Al₁/C₂N.

46

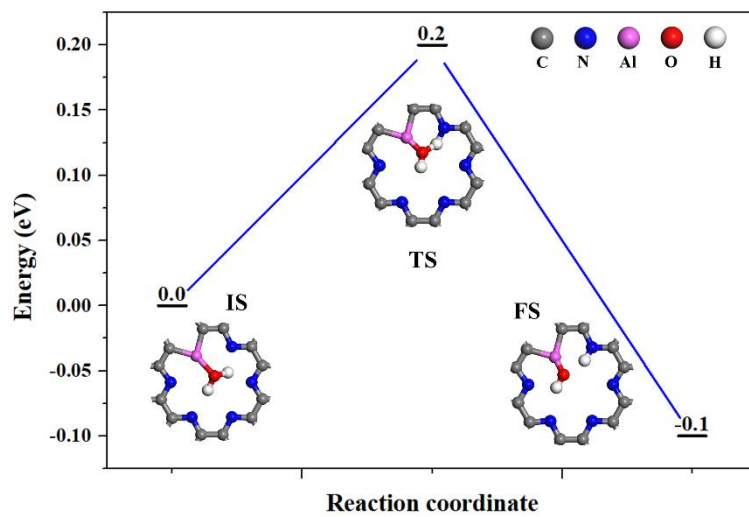


47

48

Fig. S2 Three direct oxidation pathways of HCHO on Al₁/C₂N.

49



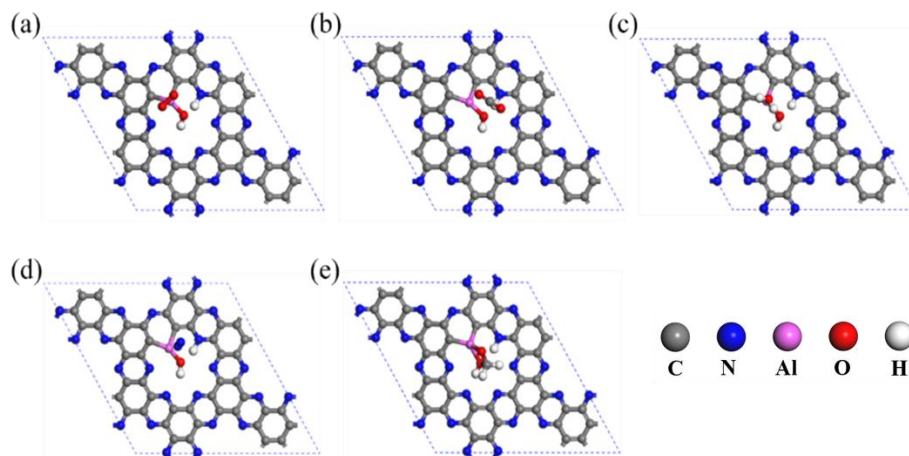
50

51

52

53

Fig. S3 The dissociating reaction of H₂O on Al₁/C₂N.



54

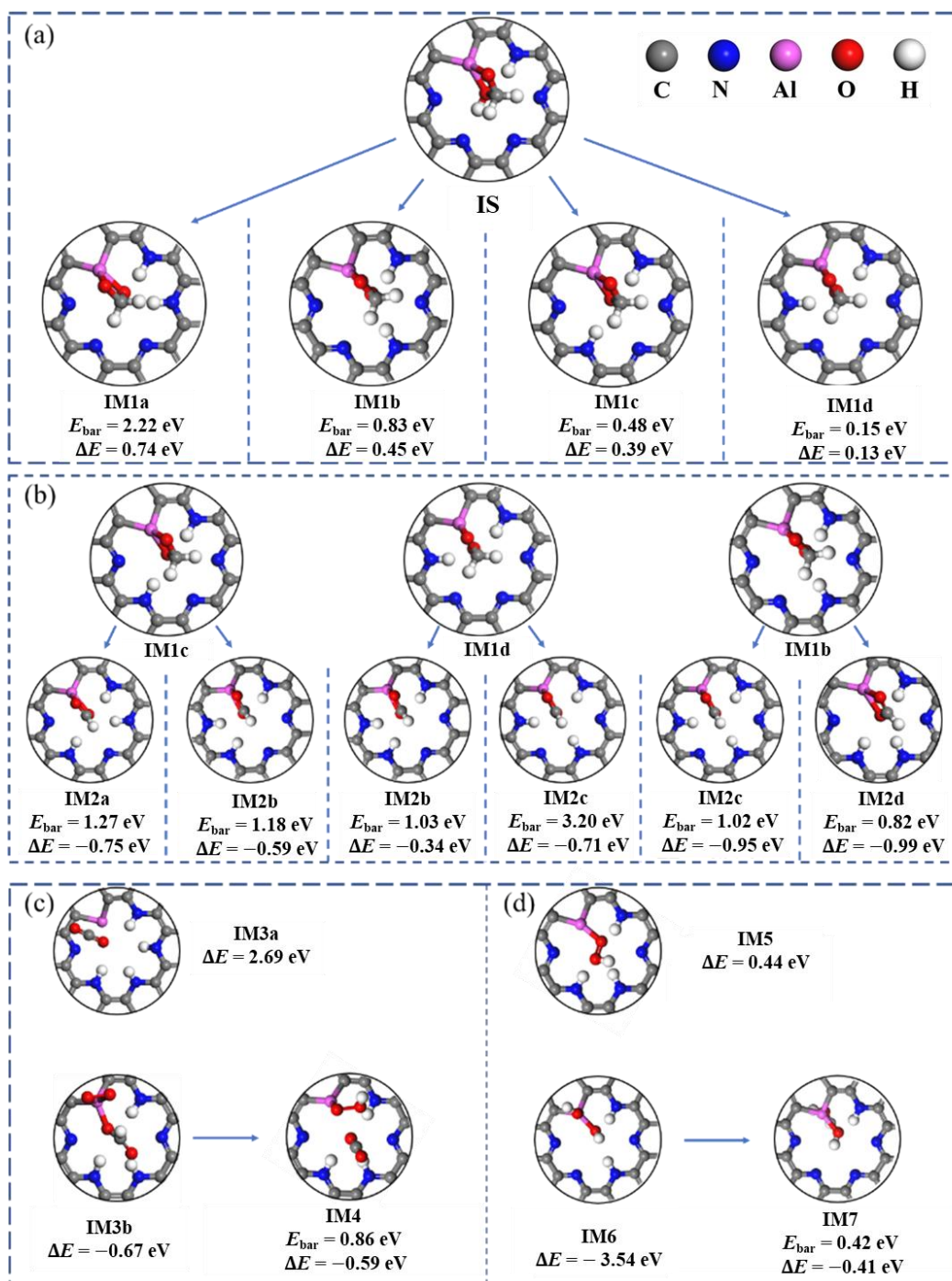
55 **Fig. S4 Most stable configurations of (a) O_2 , (b) CO_2 , (c) H_2O , (d) N_2 and (e) HCHO adsorbed**

56

on hydrated $\text{Al}_1/\text{C}_2\text{N}$.

57

58



59

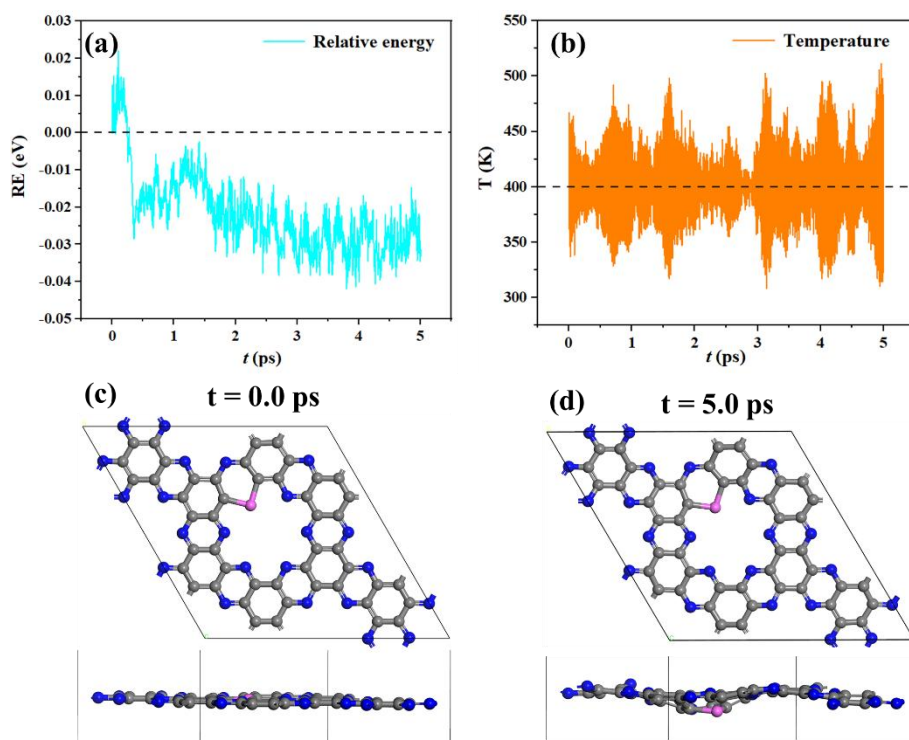
60 Fig. S5 The energy barrier (E_{bar}) and reaction energy (ΔE) of each elementary reaction of HCHO

61

degraded on hydrated $\text{Al}_1/\text{C}_2\text{N}$.

62

63



64

65

66

Fig. S6 Evolution of (a) relative energy (RE) and (b) temperature (T) of the Al₁/C₂N with NVT

67

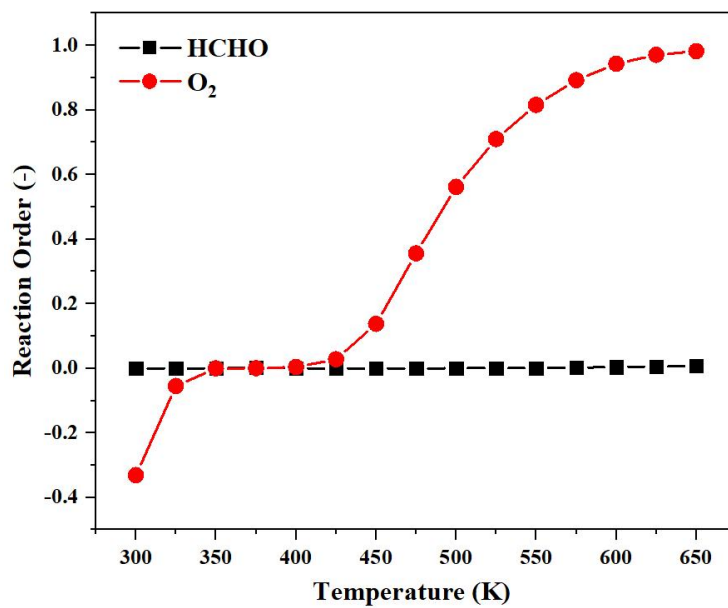
AIMD simulation time and the geometric structures of the Al₁/C₂N at simulation times (c) $t = 0$

68

ps and (d) $t = 2.5$ ps. The simulation temperature is 400 K.

69

70



71

72

Fig. S7 The reaction order of HCHO oxidation on Al₁/C₂N.

73

74

This is the end of this article!